

RESIDUAL SEISMIC PERFORMANCE OF SCALED THREE-STORY STEEL FRAMES TESTED ON A SHAKING TABLE USING THE SUBSTITUTE DAMPING MODEL

Miguel A. Diaz¹⁾, Koichi Kusunoki²⁾, and Akira Tasai³⁾

1) *PhD. Candidate, Department of Architecture and Building Science, Yokohama National University, Japan*

2) *Associate Professor, Department of Architecture and Building Science, Yokohama National University, Japan*

3) *Professor, Department of Architecture and Building Science, Yokohama National University, Japan*

miguel.ad17@gmail.com, kusunoki@ynu.ac.jp, tasai@ynu.ac.jp

Abstract: This paper compares the experimental and estimated seismic performance using the results of scaled three-story steel frames tested on a shaking table, excited with artificial and earthquake waveforms, and formulations based on the capacity spectrum method and the substitute damping model, such as the equivalent damping ratio and the response reduction ratio. For each specimen, the elastic and inelastic behavior is reproduced; in the last, the specimen was excited by the mainshock, and then the maximum expected aftershock in order to analyze the residual seismic performance.

1. INTRODUCTION

The collapse of structures, in many cases, is not caused by the mainshock, but it may be caused by the subsequent aftershocks due to the seismic capacity degradation of the building during the mainshock. Entry into a damaged building at earliest is often indispensable for different emergency reasons. Thus the estimation of the seismic performance due to the maximum expected aftershock is very much important in order to determine if the building may or may not survive.

This paper presents an instrument to conduct this estimation; it is based on the capacity spectrum method and the substitute damping model; by means of formulations, such as the equivalent damping ratio and response reduction ratio given for the life-safety limit state. This limit is established for earthquakes motions whose return period is approximately 500 years, as prescribed the Japanese Building Standard Law Enforcement Order.

The equivalent damping and response reduction ratios are prescribed by Notification No. 1457-6 (2000) of Ministry of Land, Infrastructure, Transport and Tourism of Japan (MLIT). They are used to estimate the seismic performance due to the mainshock.

On the other hand, the equation of the equivalent damping ratio for the seismic performance estimation due to aftershock proposed in previous work by Kusunoki et al. (2006) and Diaz et al. (2012) is used in this paper. Additionally, a new equation of the response reduction ratio proposed by Diaz et al. (2012) which holds good for mainshocks and aftershocks is also used.

Thus the seismic performance due to mainshocks and aftershocks from the shaking table tests are compared with the estimated seismic performance using the formulations of equivalent damping and the response reduction ratios. Ten specimens were tested under one artificial waveform and two earthquake waveforms; properties such as period, equivalent damping and response reduction ratios due to mainshocks and aftershocks are analyzed.

2. RESIDUAL SEISMIC PERFORMANCE

2.1 Aftershock assumption

The aftershock is defined as the subsequent shakes after a significant earthquake with a magnitude less than the given earthquake (mainshock).

Generally, a magnitude of the largest aftershock is smaller by 1 than that of the mainshock. The largest aftershock, in many cases, occurs within 3 days after the occurrence of the mainshock in the case of inland earthquake. As for those occurred in sea area, the largest aftershock generally occur within about 10 days (Japan Meteorology Agency).

The energy released by earthquake is proportional to its magnitude. Thus, a rough approximation may suppose that the energy released by the maximum expected aftershock is relatively close to that by the mainshock.

Therefore, if a given earthquake and its subsequent aftershocks are considered as one-long duration earthquake from the beginning of the mainshock toward the end of the maximum expected aftershock; the motion of the maximum expected aftershock can be supposed same as that of the

mainshock, then neglect the inner shakes, because they do not produce larger responses than the maximum expected aftershock.

Using this assumption, the total motion to conduct the residual seismic performance analysis is given by the earthquake inputted twice, mainshock and aftershock, and a gap between both. The duration of this gap is set in the measure that the system vibration converges to zero, as shown in Figure 1.

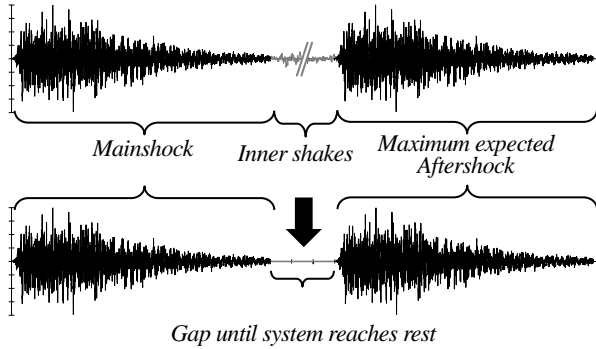


Figure 1 Aftershock assumption

2.2 Equivalent damping ratio

The equivalent damping ratio for yielding structures can be determined by the hysteresis damping in terms of the elastic strain energy of a structure by means of the geometric stiffness method (Jennings, 1968).

Notification No. 1457-6 (2000) prescribes the equivalent damping ratio ${}_m h_{eq-i}$ of a structural member i in Eq. (1) for the life-safety limit state.

$${}_m h_{eq-i} = \gamma \cdot (1 - 1/\sqrt{\mu}) \quad (1)$$

The coefficient γ in Eq. (1) is assumed as 0.25 in case of material which constitutes the member, and the joint connected to the adjacent member are rigid; and as 0.20 in cases of members or braced members where the buckling strength is degraded by the compressive forces when seismic forces acts (member exhibits a slip-type characteristic), as prescribed Notification No. 1457-6 (2000).

The coefficient γ in Eq. (1) may hold good for the estimation of the equivalent damping ratio due to mainshocks; otherwise the energy dissipation (or equivalent damping) due to the aftershock is less than or equal to that due to its corresponding mainshock. Therefore, this coefficient can be conveniently reduced in order to obtain larger responses, such as responses during an aftershock, since the response reduction ratio in Eq. (3) is inversely proportional to the equivalent damping ratio in Eq. (1). Thus, the coefficient γ is reduced to 0.12 and 0.08 by an appropriate curve fitting based on a series of nonlinear simulations obtained for systems under aftershocks (Diaz et al., 2012).

Eq. (2) is also prescribed by Notification No. 1457-6 (2000), based on the substitute structural method (Shibata and Sozen, 1976). It estimates the equivalent damping ratio of an equivalent SDOF system as the weighted average respect to the strain energy with a viscous damping ratio of 0.05 for the first-mode at the damaged-initiation limit state, since at this stage the building behavior remains elastic. ${}_m W_i$ is the strain energy dissipated in member i .

$$h_{eq} = \frac{\sum {}_m h_{eq-i} {}_m W_i}{\sum {}_m W_i} + 0.05 \quad (2)$$

2.3 Response reduction ratio

The response reduction ratio reduces the elastic spectral response to the inelastic response. Notification No. 1457-6 (2000) also prescribes the response reduction ratio as Eq. (3), which guarantees the life-safety limit state.

$$F_h = \frac{1.5}{1+10 \cdot h_{eq}} \quad (3)$$

Additionally, previous work by Diaz et al. (2012) proposes a new equation of the response reduction ratio, given by Eq. (4). It is developed solving the equation of motion under the stationary vibration, and then adapting it to the non-stationary vibration, such as earthquake motions, by means of curve fitting to analytical response of a series of nonlinear simulations.

$$F_h^* = \sqrt{\frac{1.1 + \alpha \cdot h_{eq}^2}{1 + (40 + \alpha) \cdot h_{eq}^2}} \quad (4)$$

The Japanese Building Standard Law Enforcement Order requires that spectral acceleration of a structure at a limit state should be higher than the corresponding acceleration of the reduced demand spectrum using the equivalent damping ratio at the same limit state.

2.4 Seismic performance evaluation

During a damaging earthquake, some buildings may survive, but the subsequent aftershocks may or may not cause the building collapse; that's why, it is desirable to recognize the building state (seismic performance) after a mainshock, and to estimate the seismic performance due to the maximum expected aftershock in order to anticipate if the building may or may not survive, and so safeguard life.

The seismic performance of a building due to a given earthquake motion is examined by comparing the capacity curve and demand spectrum in terms of $S_a - S_d$ relations, as shown in Figure 2. The intersection between the capacity curve and the demand spectrum for an appropriate equivalent damping ratio which represents the inelastic response under the given earthquake, is called the performance point (ATC-40, 1996).

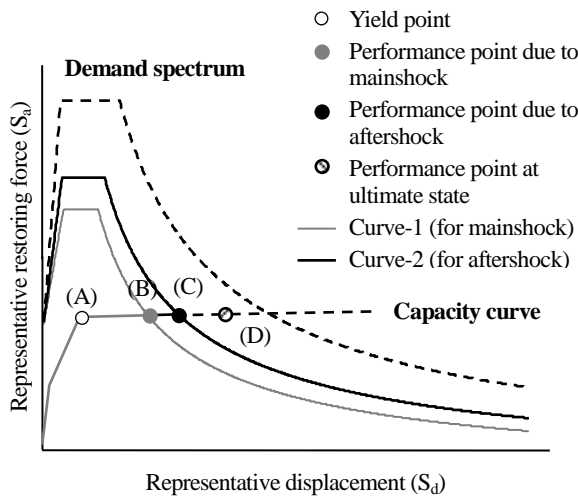


Figure 2 Scheme of the seismic performance evaluation

The concept of the seismic performance evaluation method is represented by the scheme shown in Figure 2. The performance point due to the mainshock is represented by the point (B) on the capacity curve, in this figure; the demand spectrum is reduced by increasing the viscous damping ratio until it intersects the point (B). Thus the reduced demand spectrum is represented as curve-1 in Figure 2, and the converged viscous damping ratio is defined as the equivalent damping ratio for mainshock.

The maximum response during the maximum expected aftershock, represented by the performance point (C) on the capacity curve in Figure 2, is larger than or equal to that during the mainshock, represented by the performance point (B) in the same figure. Thus the equivalent damping ratio for aftershock is less than or equal to that for mainshock, as observed in Figure 2, because the energy dissipation (or equivalent damping) during the maximum expected aftershock is less than or nearly equal to energy dissipation during its corresponding mainshock. Then the demand spectrum is again reduced until it intersects the performance point (C) in Figure 2; the reduced demand spectrum is represented as curve-2 and the converged viscous damping ratio is defined as the equivalent damping ratio for aftershock.

3. SHAKING TABLE TESTS

The experimental tests are based on the assumption described in Section 2.1. The testing program consists in four series of excitation. The first excitation was produced by the white-noise in order to evaluate the dynamic properties. The second excitation was the test using the input motion with small acceleration amplitude to induce an elastic response. The third excitation was the test using large acceleration amplitude, so that the specimen was within the inelastic range (mainshock). And, the fourth excitation was the test using the previous acceleration amplitude (or slightly less) to produce the maximum expected aftershock.

3.1 Tests specimens

The specimen consists in a scaled three-story and one-bay steel plane frames; their members are connected by bolts to a rigid joint, as shown in Figure 3.

The bay width is 1000 mm, the first-story height varies from 805 mm to 1005 mm, and the second and third stories heights are 700 mm. The beams are rectangular bars of 100×6 mm widened at the middle to support the accelerometer on each level. The first-story is constituted by rectangular bars as columns without braces; the second and third stories are braced frames with rectangular bars of 100×6 mm as columns, and circular bars M10 as braces (a pair in each front).

The design of the specimen supposed that the columns of the first-level would be only affected during the tests, due to the soft-story behavior of this structure. The sections of these columns were reduced in 50% at the bottom in order to provide to the specimen a plastic hinge to control the failure mechanism.

Thus, the properties of the specimen depend on the dimensions of first-story columns (thickness and height); the second, third braced frames are preserved for all tests. However, the second and third braced frames are also observed by the measurement system.

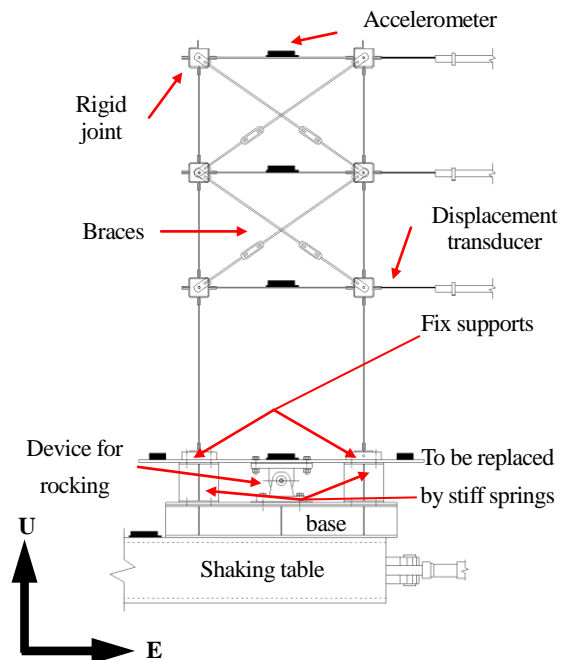


Figure 3 Configuration of specimens

The specimens Frame1a, Frame2a,b and S-F01,02,03 are fixed support; while specimens S-S01,02,03,04 are also fixed support, but the base (ground) includes a small rocking effect due to the adding of stiff springs ($K_{spring}=500 \text{ N/mm}$) between supports and base, as shown Figure 3. The initial compressive deformations of springs were 1 mm and 7 mm for S-S01,02 and S-S03,04, respectively. Members of these specimens consisted of SS400 (326 MPa). Table 1 presents characteristics of these specimens.

Table 1 Characteristics of specimens

Specimen	Thickness 1 st F column (mm)	Height 1 st F (mm)	Total weight (kN)	Natural period (s)	Yield. Disp. (mm)
Frame1 a	4.5	805	1.450	1.03	66
Frame2 a, b	4.5	1005	1.464	1.66	101
S-F 01, 02, 03	6.0	1000	1.485	0.93	71
S-S 01, 02	6.0	1000	1.485	0.99	73
S-S 03, 04	6.0	1000	1.485	0.98	73

The measurement system was given by accelerometers at the base and beams of each level, and displacement transducers connected at each eastern rigid joint, as shown in Figure 3.

3.2 Input waveforms

The input motions to conduct this study were one artificial wave: the WG60, and two earthquake records: the KOBE-NS (Kobe, 1995) and the MYG013 (Tohoku, 2011). The input motions were scaled in order to induce different performance levels on the specimen within elastic and inelastic ranges, both mainshocks and aftershocks. Figure 4 shows the WG60, the KOBE-NS and the MYG013 waveforms.

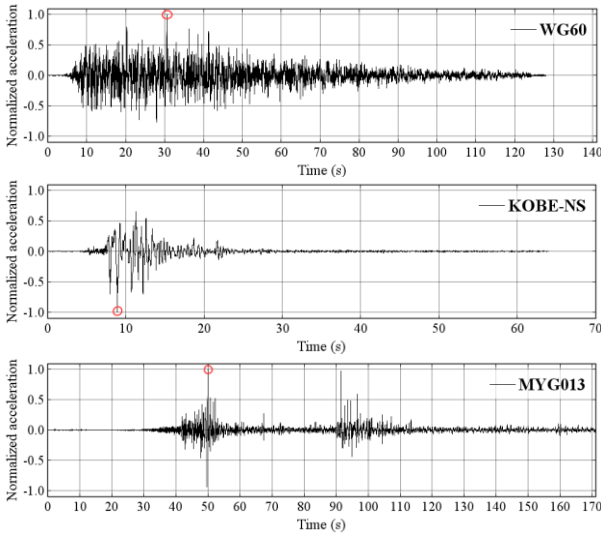
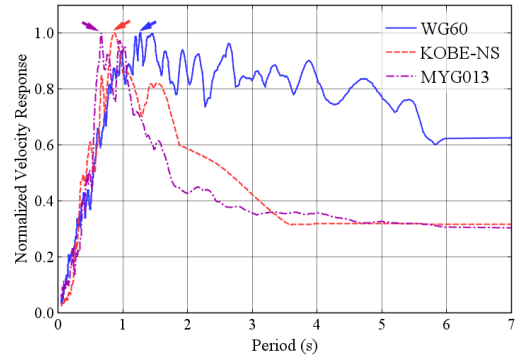
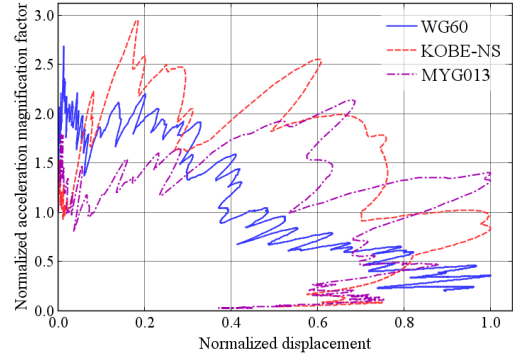


Figure 4 Input waveforms

Figure 5 shows their respective a) normalized velocity response spectra respect to the maximum spectral velocity, and b) normalized response spectra respect to peak ground acceleration (PGA) and maximum spectral displacement. The maximum spectral response with viscous damping ratio of 0.05 was obtained at periods of 1.27 seconds, 0.87 seconds and 0.67 seconds for the WG60, the KOBE-NS and the MYG013 waveforms, respectively (Figure 5a).



a) Velocity response spectra



b) Displacement and acceleration response spectra

Figure 5 Response spectra

3.3 Equivalent SDOF

In order to conduct the residual seismic performance analysis, it is necessary to transform the capacity curve of the specimen in terms of $S_a - S_d$ relations.

The probable value of the maximum response is usually given by the square root of the sum of square (SRSS) of the maximum modal response components. Then the maximum displacement at i -th story and the base shear force can be expressed approximately by Eq. (5) and Eq. (6) (Shibata, 2010), respectively; where ${}_s S_d$, ${}_s S_a$ is the spectral displacement and spectral acceleration for the s -th mode. The base shear force of N -DOF is given by Eq. (7).

$$|\delta_i|_{\max} \approx \sqrt{\sum_{s=1}^N |{}_s \beta \cdot {}_s u_i \cdot {}_s S_d|^2} \quad (5)$$

$$Q \approx \sqrt{\sum_{s=1}^N \{ \sum_{i=1}^N m_i \cdot {}_s \beta \cdot {}_s u_i \cdot {}_s S_a \}} \quad (6)$$

$$Q = \sum_{i=1}^N m_i \cdot (\ddot{x}_i + \ddot{x}_g) \quad (7)$$

Particularly, the specimens can be assumed as 3-DOF systems. Their configuration allows that second and third participation factor can be neglected, and the first-mode distribution can be assumed as the unit $\{ {}_1 u \} \approx \{ 1 \}$. Then Eq. (5) is rewritten as Eq. (8) to calculate the spectral acceleration, and Eq. (7) into Eq. (6) is rewritten as Eq. (9) to calculate the spectral displacement.

$${}_1S_d \approx \frac{|\delta_i|_{\max}}{s u_i} \quad (8)$$

$${}_1S_a = \frac{\sum_{i=1}^3 m_i (\ddot{x}_i + \ddot{x}_g)}{\sum_{i=1}^3 m_i} \quad (9)$$

3.4 Tests results

The representative response or spectral response is calculated by Eq. (8) and Eq. (9), using experimental data such as the displacement from transducers and the absolute acceleration from accelerometers on each level. The responses during mainshocks and aftershocks, in terms of $S_a - S_d$ relations, with different maximum acceleration amplitudes of waveforms are plotted in Figure 6, Figure 7 and Figure 8, where g is the acceleration of gravity.

Figure 6 shows the response during the WG60 waveform for four specimens, namely: Frame1a, S-F01, S-S01 and S-S04 with maximum acceleration amplitude of waveform of 0.36g, both mainshock and aftershock.

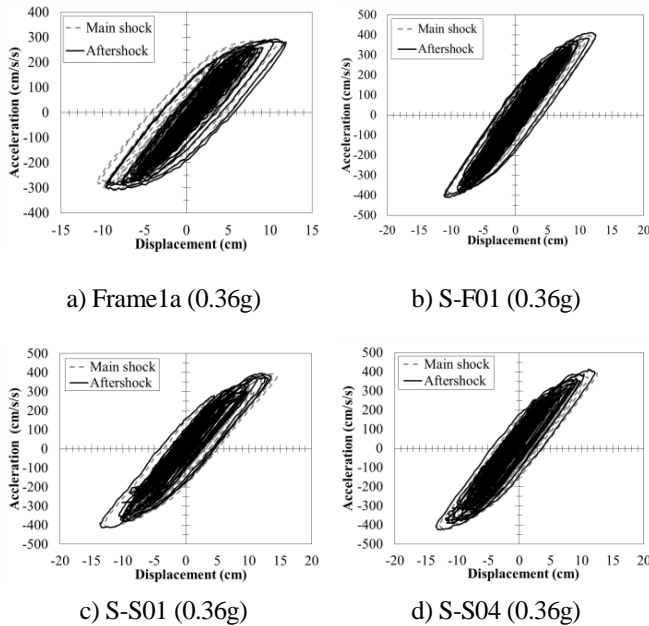


Figure 6 Response during the WG60 waveform

Figure 7 shows the response during the KOBE-NS waveform for five specimens, namely: Frame2a with maximum acceleration amplitude of waveform of 0.17g (mainshock and aftershock), Frame2b with 0.33g for mainshock and 0.25g for aftershock; and S-F02, S-S02 and S-S03 with 0.38g, both mainshock and aftershock.

In Figure 7b, a negative slope arose in the representative acceleration; it is because the specimen Frame2b is slender and long-period frame (see Table 1), and suffered the P- Δ effect (its capacity is reduced in front of the gravity effect). The maximum response within the inelastic range was larger than the elastic spectral response with damping ratio of 0.05.

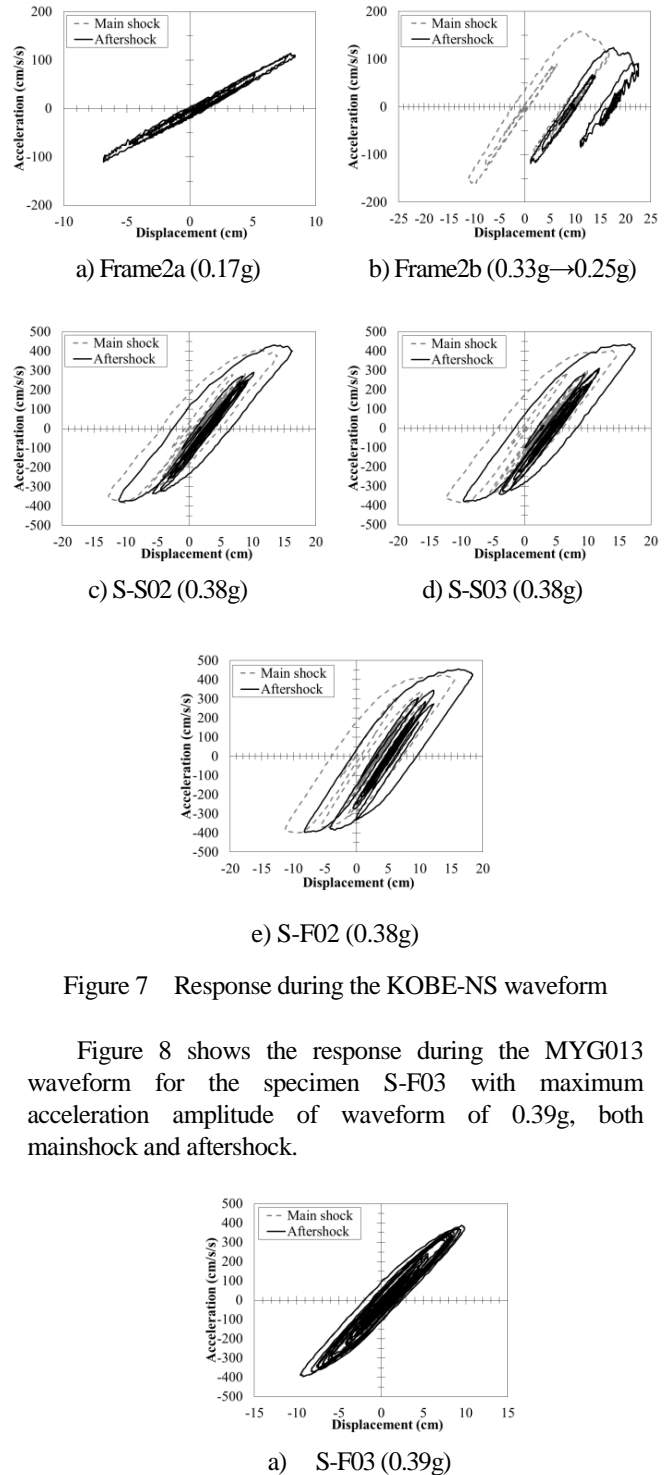


Figure 7 Response during the KOBE-NS waveform

Figure 8 shows the response during the MYG013 waveform for the specimen S-F03 with maximum acceleration amplitude of waveform of 0.39g, both mainshock and aftershock.

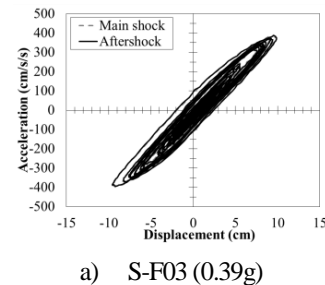


Figure 8 Response during the MYG013 waveform

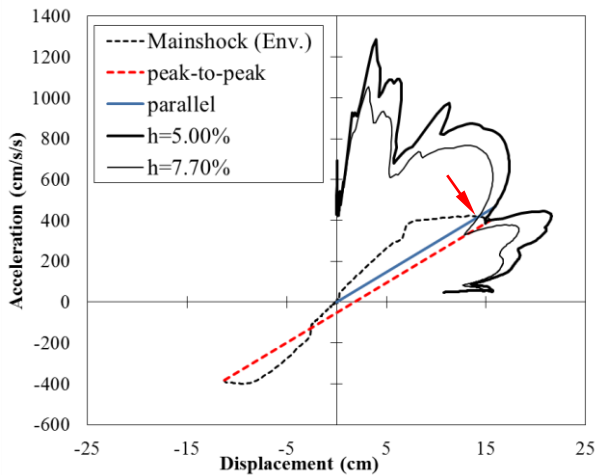
In the previous experimental study (Diaz, Kusunoki and Tasai, 2012), the equivalent damping ratio was estimated using the maximum response amplitude, negative or positive, to estimate the equivalent damping ratio; by increasing the damping ratio until the resulting demand spectrum is intersected with this maximum response amplitude, as described Section 2.4 in Figure 2.

Those results showed that some responses such as those from specimens S-F02, S-S02 and S-S03 were unsafely

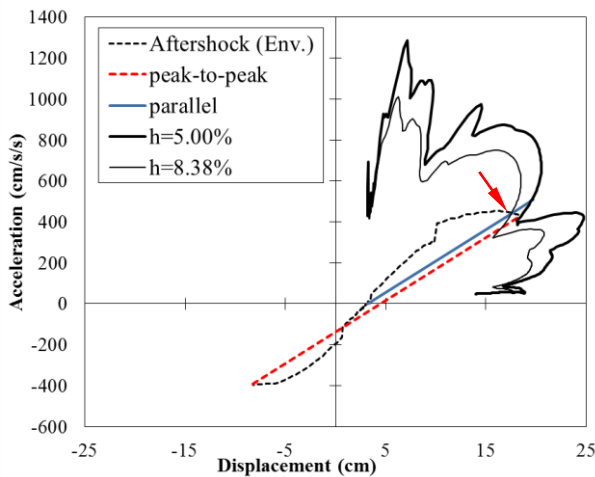
estimated using the formulations of the equivalent damping and response reduction ratios presented in this paper. It is because the fundamental period of these specimens are close to the predominant period of the corresponding input waveform (KOBE-NS). Also, the specimen Frame2b could not be used because it suffered the P- Δ effect and its maximum response amplitude is larger than the elastic spectral response with damping ratio of 0.05.

On the other hand, the equation of equivalent damping ratio given in Eq. (1) is developed by the geometric stiffness method which supposes that the positive and negative amplitudes of the hysteresis loop are equal. Although, as shown in Figure 6a, 6c, 7b, 7c, 7d and 7e, the hysteresis loops are shifted in many cases toward negative or positive direction, and amplitudes (negative and positive) turn out to be quite different; this shifting is intensified during aftershocks, where a residual deformation due to the mainshock may occur.

Thus the energy dissipation, or equivalent damping, is represented much closer to the true value when both amplitudes, negative and positive, are used to estimate an equivalent period (peak-to-peak), and then defining the equivalent amplitude.



a) Response during mainshock



b) Response during aftershock

Figure 9 Estimation of parameters using the equivalent amplitude

An important characteristic is that the envelope of the spectral response during the mainshock maintains the same shape during the aftershock, but moved toward one direction or another, and the residual deformation becomes the new origin. It means the capacity curve preserves the same shape until the structure sustains major damage (large deformation). This phenomenon can be observed in Figure 9, the envelope of the response during mainshock looks like moved toward positive direction during the aftershock, and the new origin is relocated at 3.2 cm.

Therefore, the equivalent damping and response reduction ratios are calculated after defining the equivalent amplitude as the intersection between the line parallel to the resulting line of joining the peak amplitudes (peak-to-peak) which crosses the origin and the negative or positive branch of the envelope of the spectral response (Figure 9a). In case of the response during the aftershock (Figure 9b), the parallel line crosses the new origin (residual deformation).

After defining the equivalent amplitude, the equivalent damping ratio is calculated by reducing the demand curve toward the equivalent amplitude, as describe in Section 2.4. Then the response reduction ratio is calculated as the ratio of the equivalent amplitude to the elastic response. The elastic response corresponds to the intersection between the parallel with the demand spectrum with damping ratio of 0.05, as shown in Figure 9a. In case of aftershocks, the demand spectrum is moved toward the residual deformation as shown in Figure 9b.

4. ANALYSIS OF RESULTS

Figure 10 shows the relation between the ductility factors due to mainshocks and aftershocks, using the absolute maximum displacement (maximum amplitude), and the negative and positive maximum displacement (equivalent amplitude).

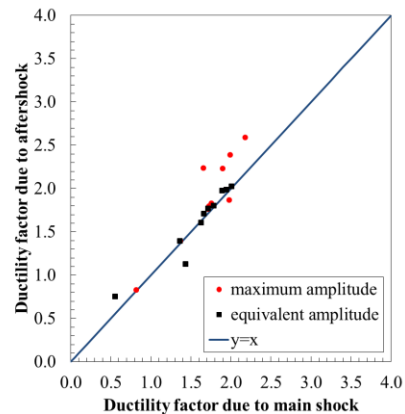


Figure 10 Relation between ductility factors

Table 2, Table 3, Table 4 and Table 5 show the ductility factor (μ), the equivalent damping ratio (h_{eq}) and the response reduction ratio (F_h) obtained from the experimental tests, and the estimated response reduction ratio. In order to

estimate the response reduction ratio, the ductility factor is evaluated into Eq. (2) to estimate the equivalent damping ratio and then it is evaluated into Eq. (3) and Eq. (4), F_h and F_h^* , respectively.

Table 2 and Table 3 show results due to mainshocks and aftershocks, respectively, using the maximum absolute displacement. As shown in these tables, the equivalent damping and response reduction ratios are not calculated for the specimen Frame-2b, because the inelastic response is much larger than the spectral response with damping ratio of 0.05, both mainshock and aftershock.

Table 2 Results due to mainshock using the maximum absolute amplitude

Specimen	waveform	Experimental			Estimated	
		μ	h_{eq}	F_h	F_h	F_h^*
Frame-1a	WG60	1.73	16.57%	0.540	0.714	0.874
Frame-2a	KOBE-NS	0.82	5.19%	0.968	1.081	1.018
Frame-2b	KOBE-NS	1.66	-	-	-	-
S-F01	WG60	1.72	11.24%	0.651	0.915	0.974
S-F02	KOBE-NS	2.18	4.42%	1.028	0.879	0.960
S-F03	MYG013	1.37	7.57%	0.770	0.935	0.981
S-S01	WG60	1.98	10.62%	0.672	0.895	0.966
S-S02	KOBE-NS	1.90	6.48%	0.907	0.890	0.964
S-S03	KOBE-NS	1.99	5.57%	0.959	0.882	0.961
S-S04	WG60	1.76	10.91%	0.665	0.897	0.967

Table 3 Results due to aftershock using the maximum absolute amplitude

Specimen	waveform	Experimental			Estimated	
		μ	h_{eq}	F_h	F_h	F_h^*
Frame-1a	WG60	1.80	16.41%	0.542	0.831	0.939
Frame-2a	KOBE-NS	0.83	4.99%	0.976	1.056	1.013
Frame-2b	KOBE-NS	2.23	-	-	-	-
S-F01	WG60	1.76	10.83%	0.671	0.905	0.970
S-F02	KOBE-NS	2.59	5.19%	1.002	0.858	0.951
S-F03	MYG013	1.39	7.37%	0.778	0.929	0.978
S-S01	WG60	1.87	10.04%	0.699	0.901	0.968
S-S02	KOBE-NS	2.23	5.95%	0.981	0.872	0.957
S-S03	KOBE-NS	2.39	5.60%	0.987	0.855	0.950
S-S04	WG60	1.83	10.07%	0.691	0.884	0.962

Table 4 and Table 5 show results due to mainshocks and aftershocks, respectively, using the equivalent amplitude defined by the positive and negative peak amplitudes (peak-to-peak). Contrasting with the maximum absolute amplitude, the equivalent amplitude allows calculating the equivalent damping and response reduction ratios for the specimen Frame-2b, which suffered P- Δ effect.

Table 4 Results due to mainshock using the equivalent amplitude

Specimen	waveform	Experimental			Estimated	
		μ	h_{eq}	F_h	F_h	F_h^*
Frame-1a	WG60	1.63	17.95%	0.525	0.735	0.887
Frame-2a	KOBE-NS	0.56	16.09%	0.639	1.305	1.044
Frame-2b	KOBE-NS	1.44	7.83%	0.885	0.984	0.996
S-F01	WG60	1.66	11.82%	0.642	0.927	0.978
S-F02	KOBE-NS	2.01	7.70%	0.892	0.892	0.965
S-F03	MYG013	1.36	7.83%	0.757	0.939	0.982
S-S01	WG60	1.79	10.99%	0.613	0.909	0.971
S-S02	KOBE-NS	1.89	6.49%	0.912	0.894	0.966
S-S03	KOBE-NS	1.95	6.19%	0.946	0.887	0.963
S-S04	WG60	1.72	11.29%	0.648	0.901	0.968

Table 5 Results due to aftershock using the equivalent amplitude

Specimen	waveform	Experimental			Estimated	
		μ	h_{eq}	F_h	F_h	F_h^*
Frame-1a	WG60	1.61	16.50%	0.498	0.855	0.950
Frame-2a	KOBE-NS	0.75	6.93%	0.886	1.084	1.019
Frame-2b	KOBE-NS	1.13	16.14%	0.698	0.985	0.996
S-F01	WG60	1.71	11.24%	0.663	0.924	0.977
S-F02	KOBE-NS	2.03	8.38%	0.870	0.890	0.964
S-F03	MYG013	1.39	7.61%	0.772	0.935	0.980
S-S01	WG60	1.80	10.80%	0.644	0.907	0.971
S-S02	KOBE-NS	1.98	5.98%	0.955	0.888	0.963
S-S03	KOBE-NS	1.98	6.70%	0.927	0.882	0.961
S-S04	WG60	1.77	10.84%	0.669	0.896	0.966

Figure 11 shows the relationship between the ductility factor and the equivalent damping ratio from the experimental test using the maximum absolute amplitude and the equivalent amplitude due to a) mainshocks and b) aftershocks.

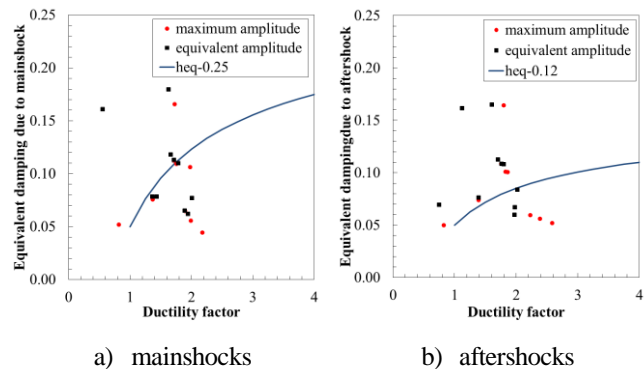


Figure 11 Estimation of equivalent damping ratio

Results in Figure 11 are compared with the estimated equivalent damping ratio which is defined by the curve heq-0.25 and heq-0.12, for mainshock and aftershock,

respectively. It corresponds to coefficients γ 0.25 and 0.12 in Eq. (1), because the hysteretic behavior is quiet close to the perfect elasto-plastic bilinear model.

The equivalent damping ratio becomes larger using the equivalent amplitude than using the maximum absolute amplitude, it is observed in Figure 11. It means that the equation of the equivalent damping ratio can be estimated more safely these values using the equivalent amplitude.

In order to compare the experimental and estimated response, the response reduction ratio is calculated from the shaking table tests and formulations. The response is safely estimated when the actual response reduction ratio (experimental) is less than or equal to the estimated response reduction ratio using the formulations presented in this paper, both mainshock and aftershock, whichever is applicable.

$$F_h^{experimental} \leq F_h^{estimated} \quad (10)$$

The comparison between the estimated response reduction ratio and the experimental response reduction ratio due to mainshocks and aftershocks is presented in Figure 12 and Figure 13, using Eq. (3) and Eq. (4), respectively. These figures show this comparison using a) the maximum absolute amplitude and b) the equivalent amplitude. Here, the response safely estimated are represented by points above the line ($y=x$).

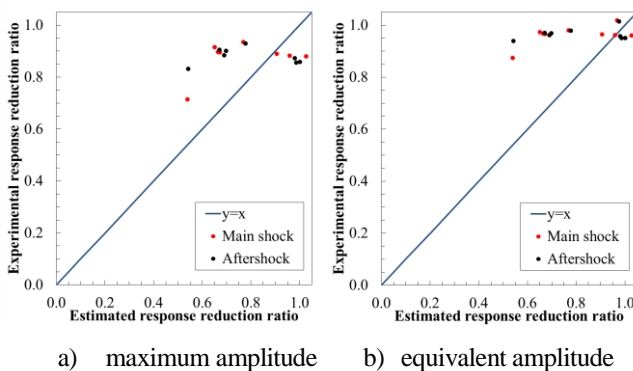


Figure 12 Response reduction ratio by F_h , Eq. (3)

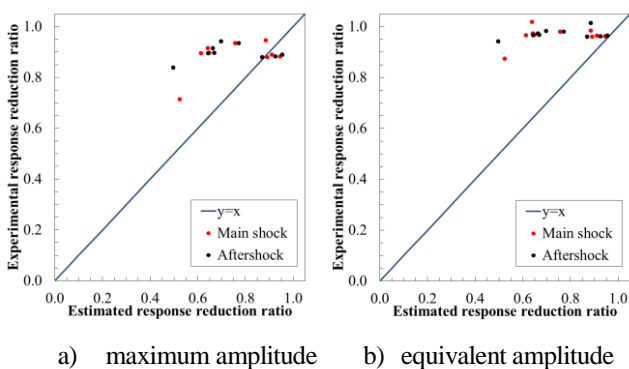


Figure 13 Response reduction ratio by F_h^* , Eq. (4)

5. CONCLUSIONS

From the analysis conducted for the experimental and estimated results, the following conclusion can be drawn:

- Ten scale three-story steel frames were tested on a shaking table, seismic performance is determined from the experimental results and compared with the estimated values.
- The definition of the equivalent amplitude allows calculating responses where the maximum absolute amplitude exceeds the elastic spectral response, even for the specimen which suffered the P- Δ effect.
- The equivalent damping ratio can be more safely estimated when the equivalent amplitude is defined instead of the maximum absolute amplitude.
- The formulations estimated safely the equivalent damping ratio and then the response reduction ratio due to mainshocks and aftershocks using the peak amplitudes to define the equivalent amplitude. The response reduction ratio is more safely estimated using Eq. (4) than Eq. (3).

However, this technique would become safer for the seismic performance estimation if an equation to estimate the shifting displacement is incorporated.

Acknowledgements:

Authors acknowledge Miho Yamashita, Yuichi Hatanaka, Daiki Hinata, and Yuki Hattori for their great contributions during the tests. The installation and maintenance of the measurement system has been supported by Mr. Masayuki Araki, Mr. Takamori Ito and other staffs of aLab Co. Also, the authors would like to express their gratitude to the Japan Science and Technology Agency (JST) through the Science and Technology Research Partnership for Sustainable Development (SATREPS) project “Enhancement of earthquake and tsunami disaster mitigation technology in Peru” for the fellowship during this research.

References:

- Ministry of Land, Infrastructure, Transport and Tourism (2000). “Notification No. 1457-6.” Technical Standard for Structural Calculation of Response and Limit Strength of Buildings.
- Jennings P. (1968). “Equivalent Viscous Damping for Yielding Structures.” *Proceedings of ASCE*, Vol.94, No. 1, 103-116.
- Kusunoki, K. (2006) “Analytical Study on Estimation of Equivalent Viscous Damping Ratio for aftershock”, *Proceedings of the Japan Concrete Institute Proceedings of the Japan Concrete Institute* 28(2), 1057-1062.
- Diaz M., Kusunoki K. and Tasai A. (2012). “Analytical Study of Residual Seismic Performance by Estimation of Response Reduction Ratio and Equivalent Damping for Aftershocks.” *Proceedings of 15th World Conference on Earthquake Engineering*, Paper ID 1950.
- Shibata A. and Sozen M. (1976). “The Substitute Structure Method for Seismic Design in RC.” *Proceedings of ASCE, Journal on Structural Division*, Vol. 102, No. 1, 1-18.
- ATC-40 (1996). Seismic Evaluation and Retrofit of Concrete Buildings, Report No. SS 96-01, Applied Technology Council.
- Shibata A. (2010). “Dynamic Analysis of Earthquake Resistant Structures”, Tohoku University Press.
- Diaz M., Kusunoki K. and Tasai A. (2012). “Experimental Study on Residual Seismic Performance of Scaled Three-Story Steel Frames Tested on a Shaking Table.” *Proceedings of International Symposium on Earthquake Engineering*, 349-356.